

Article

Synthesis and Spectroscopic Properties of Selected Acrylic and Methacrylic Derivatives of 2-Mercaptobenzothiazole

Janina Kabatc-Borc ¹, Przemysław Czeleń ² and Agnieszka Skotnicka ^{1,*}

¹ Faculty of Chemical Technology and Engineering, Bydgoszcz University of Science and Technology, Seminaryjna 3, 85-326 Bydgoszcz, Poland

² Department of Physical Chemistry, Faculty of Pharmacy, Collegium Medicum, Nicolaus Copernicus University, Kurpińskiego 5, 85-096 Bydgoszcz, Poland

* Correspondence: askot@pbs.edu.pl; Tel.: +48-523749111

Abstract: One of the most basic properties of chemical compounds is structural symmetry or asymmetry. This property can be considered at different levels of structural organization. The physical, chemical, biological, and technological properties of organic compounds depend on their chemical structure and are systematically related to it. The presented paper is focused on the synthesis and study of the spectroscopic properties of selected photoinitiators from the acrylate and methacrylate derivatives of 2-(benzothiazolylthio)ethyl. The indicated compounds can find potential application in medicine. The 2-(benzothiazolylthio)ethyl acrylate and methacrylate derivatives were characterized using infrared spectroscopy (IR) and nuclear magnetic resonance (NMR) spectroscopy. Their spectroscopic properties were determined on the basis of UV–Vis spectra. The calculated DFT energies and Frontier Molecular Orbitals calculations of the studied compounds were proved to be consistent with the experimental observations. The results have showed that the introduction of the ethoxy substituent increases the reactivity of the compounds and results in the slight bathochromic shift (~19 nm) of the absorption spectra maxima.

Keywords: 2-mercaptobenzothiazole; synthesis; spectroscopic properties; quantum chemical calculations; molecular asymmetry



Citation: Kabatc-Borc, J.; Czeleń, P.; Skotnicka, A. Synthesis and Spectroscopic Properties of Selected Acrylic and Methacrylic Derivatives of 2-Mercaptobenzothiazole. *Symmetry* **2023**, *15*, 370. <https://doi.org/10.3390/sym15020370>

Academic Editor: Stefano Superchi

Received: 29 December 2022

Revised: 18 January 2023

Accepted: 26 January 2023

Published: 30 January 2023



Copyright: © 2023 by the authors. Licensee MDPI, Basel, Switzerland. This article is an open access article distributed under the terms and conditions of the Creative Commons Attribution (CC BY) license (<https://creativecommons.org/licenses/by/4.0/>).

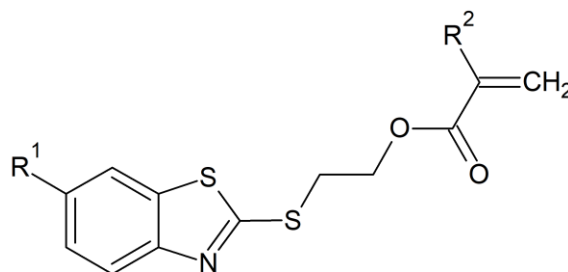
1. Introduction

Multifunctional polymeric materials play a key role in many biomedical technologies [1,2]. A wide range of different polymers is available and their advantages include the possibility of modifying physical, chemical, and biological properties over a wide range to match the requirements of specific applications. Due to the very advanced mechanical properties that can be observed, for example, in polymers with shape memory that, under the influence of a special stimulus, such as pH, temperature, magnetic field, or light, can freely deform and return to their original shape, such polymers are used in many biomedical applications. Other medical applications of polymers are drug delivery reservoirs [3], hemodialysis membranes, [4] extracorporeal membrane oxygenation [5], and dental restorative materials. Synthetic polymers have gained a strong appeal for medical applications in temporary in vivo applications such as vascular catheters [5], urinary catheters [6], ureteral stents [7], or wound dressings [8]. Polymer research in the field of biomedicine includes not only general surgical implants, such as suture materials [9], tissue adhesives and sealants [10], surgical meshes [11], but also surgical implants [11]. The numerous types of polymers that are currently in use in all fields of medicine include plastic, reconstructive, and cosmetic surgery [12], ophthalmology [13], dentistry [14], and neurosurgery [14].

Synthetic polymers gained high attraction for technical as well as for medical application for various reasons. A wide range of physical and chemical properties can be achieved

based on the monomer units, polymerization reaction, and formation of co-polymers consisting of different components at adjustable concentrations [15]. Synthetic methodologies that have enabled the production of well-defined and functionalized polymers play a key role in this research area. In this study, a light-sensitive photoinitiator (meth)acrylic of 2-mercaptobenzothiazole derivatives with different substituents were designed and synthesized. According to the literature, some of these compounds can act not only as photoinitiators but also as attractive building blocks and components of advanced polymer materials characterized by a high refractive index, for optical, e.g., as foldable intraocular lenses [16], and for industrial applications (coatings) [17,18].

All properties of organic molecules, physical, chemical, biological, and technological, depend on their chemical structure and vary with it in a systematic way. Structural symmetry and asymmetry are one of many contributing factors that need to be considered when designing of new compounds. By modifying the structure of the compound, such as by introducing an appropriate substituent, its photophysical properties can be easily modified to meet the high demand of various applications. The study of structural correlations with spectroscopic properties of the newly synthesized compounds is one of the goals of the presented work. In the present research, four photoinitiators with a hydrogen atom or ethoxy group (Scheme 1) in the 6-position of the aromatic ring of 2-mercaptobenzothiazole were synthesized. Their structures were confirmed using Nuclear Magnetic Resonance (NMR) and Attenuated Total Reflectance Spectroscopy (ATR-FTIR). Additionally, their photophysical and photochemical properties were determined using UV-Vis absorption spectroscopy. It should be highlighted that not only the influence of the substituent was investigated. It was also determined how the modification of an acrylic derivative to a methacrylic derivative (Scheme 1) affects the synthesis and properties of the new compounds. The obtained experimental data were compared and supported by the results of appropriate quantum chemical calculations.



where: $R^1/R^2 = H$ (1); $R^1 = 6\text{-OEt}$, $R^2 = H$ (2); $R^1 = H$, $R^2 = CH_3$ (3); $R^1 = 6\text{-OEt}$, $R^2 = CH_3$ (4)

Scheme 1. Structure of 2-(benzothiazolylthio)ethyl acrylate and methacrylate derivatives.

2. Materials and Methods

2.1. Materials

All the reagents and solvents were purchased from Sigma-Aldrich (Poznań, Poland) and used without further purification. The highest ($\geq 99\%$) purity of all the used chemicals was required for the spectroscopic studies.

2.2. Synthesis

2.2.1. Synthesis of 2-(2-Benzothiazolylthio)ethyl Acrylate and Methacrylate Derivatives

2-(Benzothiazolylthio)ethyl Acrylate (1) [17] It was synthesized in two steps according to procedure [16]: Chloroethanol (0.09 mol, 6 mL) was added to a solution of 2-mercaptobenzothiazole (0.06 mol, 10 g), potassium hydroxide (0.09 mol, 5 g), and potassium iodide (0.003 mol, 0.5 g) in 100 mL ethanol/water (1:1) mixture. The reaction medium was refluxed overnight. Then, the ethanol was evaporated and 70 mL of dichloromethane and 50 mL of 5% NaOH solution were added to the residue. The organic layer was extracted

using dichloromethane and dried over MgSO_4 . The dichloromethane was evaporated. The crude, brown oil was purified using silica gel column chromatography with hexane/ethyl acetate (7:3) as an eluent. 2-(2-Benzothiazolylthio)ethanol (a white solid) was obtained with a reaction yield of 61% and m.p. 50–53 °C.

The second step: For a solution of 2-(2-benzothiazolylthio)ethanol (the product of the first step) (23 mmol, 3.85 g) and triethylamine (34 mmol, 4.81 mL) in 38 mL anhydrous dichloromethane at 0 °C, acryl chloride (34 mmol, 2.8 mL) was added dropwise over a period of 30 min. The content of the reaction vessel was allowed to proceed for 3 h at this temperature. Then, an aqueous solution of 5% NaOH was added and the reaction product was extracted using dichloromethane. MgSO_4 was added to the organic layer to become involved in the residual water. The dichloromethane was evaporated. The crude, yellow oil was purified using silica gel column chromatography with dichloromethane as an eluent (fractions were collected at 300 nm). 2-(Benzothiazolylthio)ethyl acrylate (1) (a yellow oil) was obtained with a reaction yield of 52%.

2-(2-(6-Ethoxybenzothiazolylo)thio)ethyl Acrylate (2) [17] It was synthesized in two steps according the following procedure [16]: for a solution of 6-ethoxy-2-mercaptobenzothiazole (0.06 mol, 12.67 g), potassium hydroxide (0.09 mol, 5 g), and potassium iodide (0.003 mol, 0.5 g) in a 100 mL ethanol/water (1:1) mixture, chloroethanol (6 mL) was added. The reaction medium was refluxed overnight. Then, the ethanol was evaporated and 70 mL of dichloromethane and 50 mL of 5% NaOH solution were added to the residue. The organic layer was extracted using dichloromethane and dried over MgSO_4 . The dichloromethane was evaporated. The crude solid was recrystallized from ethanol. 2-(6-Ethoxy-2-benzothiazolylthio)ethanol (a white solid) was obtained with a reaction yield of 79% and m.p. 85.5–86.5 °C.

The second step: For a solution of 2-(6-ethoxy-2-benzothiazolylthio)ethanol (the product of the first step) (23 mmol, 5.87 g) and triethylamine (34 mmol, 4.81 mL) in 38 mL anhydrous dichloromethane at 0 °C, acryl chloride (34 mmol, 2.8 mL) was added dropwise over a period of 30 min. The content of the reaction vessel was allowed to proceed for 3 h at this temperature. Then, an aqueous solution of 5% NaOH was added and the reaction product was extracted using dichloromethane. MgSO_4 was added to the organic layer to become involved in the residual water. The dichloromethane was evaporated. The crude, yellow oil was purified using silica gel column chromatography with dichloromethane as an eluent (fractions were collected at 300 nm). 2-(6-Ethoxybenzothiazolylthio)ethyl acrylate (2) (a transparent oil) was obtained with a reaction yield of 66%.

2-(Benzothiazolylthio)ethyl Methacrylate (3) [16,18] It was synthesized according to the literature guidelines [18] and with the modification procedure of purification: for 2-mercaptobenzothiazole (28 mmol, 4.68 g) and sodium bicarbonate (28.5 mol, 2.4 g) in 10 mL dimethylformamide at 60 °C, 2-chloroethyl methacrylate (29 mmol, 2.93 mL) was added dropwise. The reaction medium was refluxed overnight. Then, the reaction medium was washed with an aqueous solution of 5% NaOH and extracted using diethyl ether. The top organic layer was separated, dried over MgSO_4 , filtered, and stripped of solvent under vacuum. The crude, yellow oil was purified using silica gel column chromatography with dichloromethane as an eluent (fractions were collected at 300 nm). The resulting oil was extracted using methyl alcohol to afford 2-(benzothiazolylthio)ethyl methacrylate (3) as a pale-yellow oil with a reaction yield of 38%.

2-(2-(6-Ethoxybenzothiazolylo)thio)ethyl Methacrylate (4) It was synthesized according to the method described by [18] and with the modification procedure of purification: for 6-ethoxy-2-mercaptobenzothiazole (28 mmol, 5.91 g) and sodium bicarbonate (28.5 mol, 2.4 g) in 10 mL dimethylformamide at 60 °C, 2-chloroethyl methacrylate (29 mmol, 2.93 mL) was added dropwise. The reaction medium was refluxed overnight. Then, the reaction medium was washed with an aqueous solution of 5% NaOH and extracted using diethyl ether. The top organic layer was separated, dried over MgSO_4 , filtered, and stripped of solvent under vacuum. The crude, brown oil was purified using silica gel column chromatography with dichloromethane as an eluent (fractions were collected at 296 nm). Finally,

the product was recrystallized from methanol. 2-(2-(6-Ethoxybenzothiazolyl)thio)ethyl methacrylate (**4**) (white solid) was obtained in a 45% reaction yield and m.p. 45–46 °C.

2.2.2. Elemental Analysis Is as Follows

2-(Benzothiazolylthio)ethyl Acrylate (**1**) IR (ATR), cm^{-1} : 3020–3435, 2889–2985, 1720, and 1633. ^1H NMR (400 MHz, CDCl_3) δ (ppm): 7.18 (d, 1H, $^3J_{\text{H,H}} = 7.78$ Hz, Ar), 7.76 (d, 1H, $^3J_{\text{H,H}} = 7.74$ Hz, Ar), 7.33 (dt, 1H, Ar), 7.20 (dt, 1H, Ar), 6.35 (d, 1H, $^3J_{\text{H,H}} = 17.28$ Hz, $\text{CH}=\text{CH}_2$), 6.04 (q, 1H, $\text{CH}=\text{CH}_2$), 5.75 (d, 1H, $^3J_{\text{H,H}} = 10.44$ Hz, $\text{CH}=\text{CH}_2$), 4.46 (t, 2H, $\text{CH}_2\text{-O}$), and 3.53 (t, 2H, S-CH_2). ^{13}C NMR (100 MHz, CDCl_3) δ (ppm): 165.8, 165.6, 152.9, 135.6, 131.4, 128.0, 126.1, 124.4, 121.6, 121.0, 62.7, and 31.8. $\text{C}_{12}\text{H}_{11}\text{NO}_2\text{S}_2$, Calcd. C, 54.32, H, 4.18, N, 5.28, and S, 24.17. Found C, 54.02, H, 4.38, N, 5.18, and S, 27.37.

2-(2-(6-Ethoxybenzothiazolyl)thio)ethyl Acrylate (**2**) IR (ATR), cm^{-1} : 3035–3434, 2880–2978, 1721, and 1634. ^1H NMR (400 MHz, CDCl_3) δ (ppm): 7.67 (d, 1H, $^3J_{\text{H,H}} = 8.70$ Hz, Ar), 7.14 (s, 1H, Ar), 6.93 (dd, 1H, Ar), 6.34 (d, 1H, $^3J_{\text{H,H}} = 17.36$ Hz, $\text{CH}=\text{CH}_2$), 6.04 (q, 1H, $\text{CH}=\text{CH}_2$), 5.76 (d, 1H, $^3J_{\text{H,H}} = 10.42$ Hz, $\text{CH}=\text{CH}_2$), 4.46 (t, 2H, $\text{CH}_2\text{-O}$), 3.99 (q, 2H, $-\text{OCH}_2\text{CH}_3$), 3.55 (t, 2H, S-CH_2), and 1.37 (t, 3H, $-\text{OCH}_2\text{CH}_3$). ^{13}C NMR (100 MHz, CDCl_3) δ (ppm): 165.8, 162.1, 156.5, 147.4, 136.6, 131.3, 128.0, 122.0, 115.4, 104.8, 64.1, 62.8, 32.0, and 14.8. $\text{C}_{14}\text{H}_{15}\text{NO}_3\text{S}_2$, Calcd. C, 54.35, H, 4.89, N, 4.53, and S, 20.73. Found C, 54.40, H, 4.84, N, 4.40, and S, 20.86.

2-(Benzothiazolylthio)ethyl Methacrylate (**3**) IR (ATR), cm^{-1} : 3060, 2890–2953, 1714, and 1635. ^1H NMR (400 MHz, CDCl_3) δ (ppm): 7.80 (d, 1H, Ar), 7.67 (d, 1H, Ar), 7.34 (dt, 1H, Ar), 7.23 (dt, 1H, Ar), 6.04 (s, 1H, $\text{C}(\text{CH}_3)=\text{CH}_2$), 5.48 (s, 1H, $\text{C}(\text{CH}_3)=\text{CH}_2$), 4.46 (t, 2H, $\text{CH}_2\text{-O}$), 3.61 (t, 2H, S-CH_2), and 1.84 (t, 1H, CH_3). ^{13}C NMR (100 MHz, CDCl_3) δ (ppm): 167.0, 165.7, 152.9, 135.9, 135.2, 126.1, 126.1, 124.6, 121.6, 121.0, 62.8, 31.9, and 18.2. $\text{C}_{13}\text{H}_{13}\text{NO}_2\text{S}_2$, Calcd. C, 55.89, H, 4.69, N, 5.01, and S, 22.95. Found C, 55.74, H, 4.74, N, 5.16, and S, 22.90.

2-(2-(6-Ethoxybenzothiazolyl)thio)ethyl Methacrylate (**4**) IR (ATR), cm^{-1} : 3078–3408, 2894–2976, 1710, and 1635. ^1H NMR (400 MHz, CDCl_3) δ (ppm): 7.74 (d, 1H, $^3J_{\text{H,H}} = 8.92$ Hz, Ar), 7.14 (s, 1H, Ar), 6.96 (dd, 1H, Ar), 6.03 (s, 1H, $\text{C}(\text{CH}_3)=\text{CH}_2$), 5.49 (s, 1H, $\text{C}(\text{CH}_3)=\text{CH}_2$), 4.46 (t, 2H, $\text{CH}_2\text{-O}$), 4.00 (q, 2H, $-\text{OCH}_2\text{CH}_3$), 3.62 (t, 2H, S-CH_2), 1.85 (s, 1H, CH_3), and 1.38 (t, 3H, $-\text{OCH}_2\text{CH}_3$). ^{13}C NMR (100 MHz, CDCl_3) δ (ppm): 167.1, 162.6, 156.7, 146.9, 136.3, 135.9, 126.1, 121.9, 115.5, 104.8, 64.2, 63.0, 32.2, 18.2, and 14.8. $\text{C}_{15}\text{H}_{17}\text{NO}_3\text{S}_2$, Calcd. C, 55.70, H, 5.30, N, 4.33, and S, 19.83. Found C, 55.56, H, 5.24, N, 4.48, S, and 19.98.

2.3. Experimental Measurements

2.3.1. NMR Measurements

The ^1H and ^{13}C NMR spectra were recorded using an Ascend III spectrometer operating at 400 MHz, Bruker. Chloroform was used as a solvent and tetramethylsilane (TMS) as the internal standard. The chemical shifts (δ) are reported in ppm relative to TMS and coupling constants (J) in Hz.

2.3.2. Elemental Analysis Measurements

The elemental analysis was conducted with a Vario MACRO 11.45–0000, Elemental Analyser System GmbH, (Toruń, Poland) operating with the VARIOEL software (version 5.14.4.22).

2.3.3. The Melting Point Measurements

The melting point was measured on the Melting Point M-565 Apparatus (Buchi) (Bydgoszcz, Poland) with a measuring speed of 5 °C/min.

2.3.4. UV–Vis Measurements

The absorption spectra were measured at room temperature in a quartz cuvette (1 cm) using an Agilent Technology UV–Vis Cary 60 Spectrophotometer (Bydgoszcz, Poland).

2.3.5. FT-IR Measurements

The infrared spectra were recorded using reflectance spectroscopy measurements realized using Alpha Bruker's compact FT-IR spectrometer and a spectrophotometer equipped with diamond ATR in the range of 4000–360 cm^{-1} (Bydgoszcz, Poland).

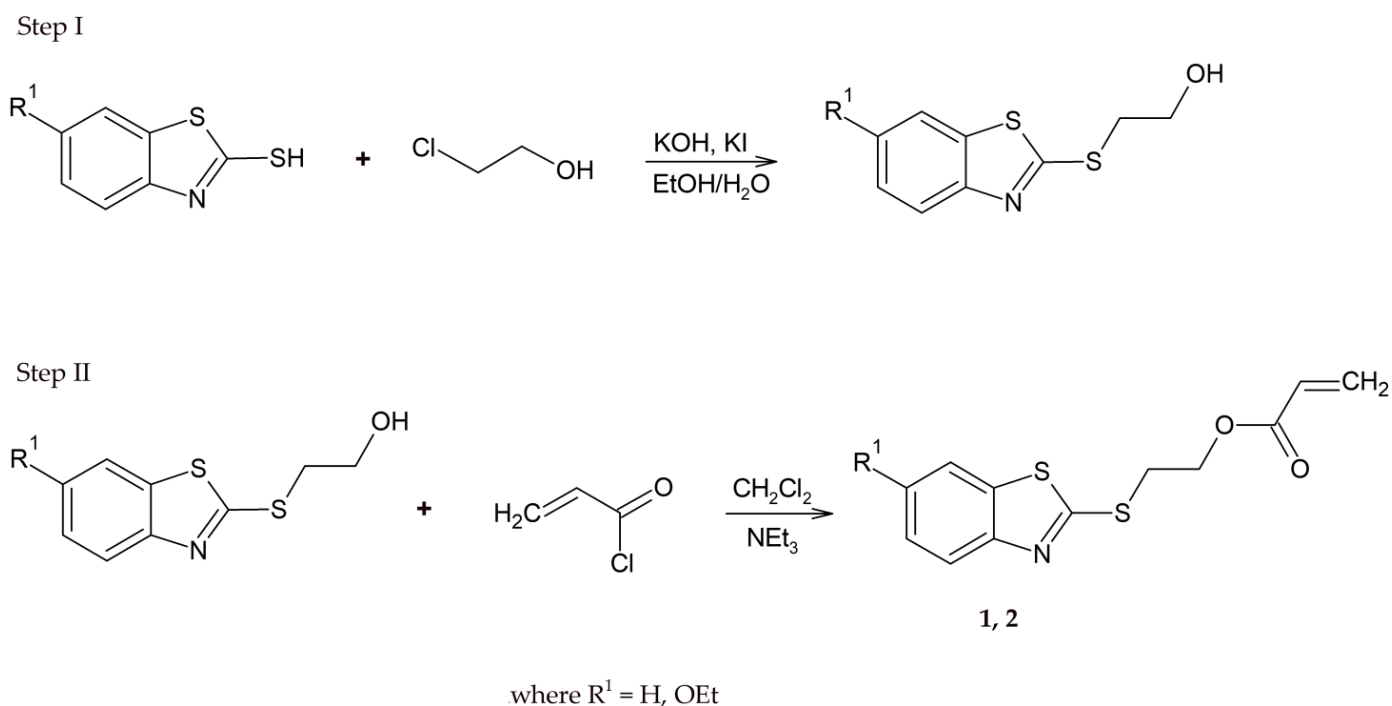
2.3.6. Quantum-Mechanical Calculations

The geometry optimization, vibrational spectra, and the Highest Occupied Molecular Orbital (HOMO) and Lowest Unoccupied Molecular Orbital (LUMO) energies were calculated based on density functional theory with the use of B3LYP [19–21] functional and 6-311+G(d,p) basis set [22,23]. All the calculations were carried out using Gaussian 09 software [24]. The analysis of the frontier orbitals and FT-IR spectra including the extraction of frequencies and a visual presentation of the vibrational modes and orbitals was realized with the use of the Avogadro 1.2.0 application [25].

3. Results and Discussion

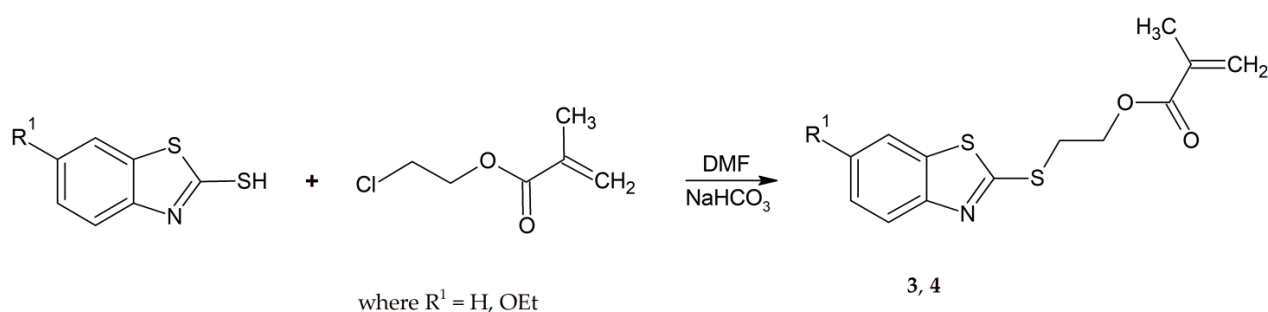
3.1. Synthesis and NMR Data

In recent years, several methods have been reported for the synthesis of acrylate and methacrylate derivatives of 2-mercaptobenzothiazole [16–18,26]. The treatment of 2-mercaptobenzothiazole with chloroethanol in the presence of potassium hydroxide and potassium iodide causes its transformation into 2-(2-benzothiazolylthio)ethanol. The purified intermediate product was always used in the subsequent synthetic step. The second step involved the esterification of 2-(2-benzothiazolylthio)ethanol with acrylate chloride (Scheme 2).



Scheme 2. The synthesis procedure of 2-(2-benzothiazolylthio)ethyl acrylate derivatives (1, 2).

The 2-(2-benzothiazolylthio)ethyl methacrylate derivatives (3, 4) were synthesized in one step by refluxing the 2-mercaptobenzothiazole with 2-chloroethyl methacrylate (Scheme 3).



Scheme 3. The synthesis procedure of 2-(2-benzothiazolylthio)ethyl methacrylate derivatives (3, 4).

The structures of the newly synthesized compounds were confirmed using nuclear magnetic resonance spectroscopy. The most characteristic ¹H and ¹³C NMR chemical shifts data were presented in Tables 1 and 2, respectively. The ¹H-NMR signals of =CH₂ of 2-(benzothiazolylthio)ethyl acrylate (1) and 2-(2-(6-ethoxybenzothiazolyl)thio)ethyl acrylate (2) can be seen at δ = 5.75–6.35 ppm in CDCl₃, which are a doublet. The same protons of 2-(benzothiazolylthio)ethyl methacrylate (3) and 2-(2-(6-ethoxybenzothiazolyl)thio)ethyl methacrylate (4) can be found at δ = 5.75–6.35 ppm in CDCl₃, but as a singlet. The remaining protons attached to the carbon atoms involved in the carbon–carbon double bond were observed at 6.04 ppm as a quartet. The alkyl protons of the CH₂ groups appeared at about 4.5 ppm and 3.5 ppm for CH₂-O and CH₂-S, respectively. In each case, they were triplets.

Table 1. ¹H NMR chemical shifts of 2-(2-benzothiazolylthio)ethyl acrylate (1, 2) and methacrylate (3, 4) derivatives for 0.1–0.2 M Solution CDCl₃ (measured) and CDCl₃, DMSO-d₆ (italic, calculated) at 303 K.

Compound	Solvent	CH=CH ₂ /C(CH ₃)=CH ₂	CH=CH ₂	C(CH ₃)=CH ₂	CH ₂ -O	S-CH ₂
1	CHCl ₃	6.35; 5.75	6.04	-	4.46	3.53
	<i>CHCl₃</i>	7.05; 6.30	6.53	-	4.37	3.48
	<i>DMSO-d₆</i>	7.04, 6.37	6.59	-	4.40	3.53
2	CHCl ₃	6.34, 5.76	6.04	-	4.46	3.55
	<i>CHCl₃</i>	7.03; 6.29	6.51	-	4.35	3.43
	<i>DMSO-d₆</i>	7.02, 6.36	6.59	-	4.44	3.53
3	CHCl ₃	6.04, 5.48	-	1.84	4.46	3.61
	<i>CHCl₃</i>	6.78; 5.98	-	1.93	4.36	3.51
	<i>DMSO-d₆</i>	6.70, 6.04	-	2.02	4.39	3.58
4	CHCl ₃	6.03, 5.49	-	1.85	4.46	3.62
	<i>CHCl₃</i>	6.76; 5.94	-	1.97	4.32	3.46
	<i>DMSO-d₆</i>	6.75, 6.02	-	1.94	4.26	3.56

Table 2. ¹³C NMR chemical shifts of 2-(2-benzothiazolylthio)ethyl acrylate (1, 2) and methacrylate (3, 4) derivatives for 0.1–0.2 M solutions in CDCl₃ (measured) and CDCl₃, DMSO-d₆ (italic, calculated) at 303 K.

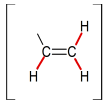
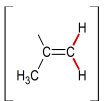
Compound	Solvent	CH=CH ₂ /C(CH ₃)=CH ₂	CH=CH ₂ /C(CH ₃)=CH ₂	C=O	CH ₂ -O	S-CH ₂
1	CHCl ₃	135.3	131.4	165.8	62.7	31.8
	<i>CHCl₃</i>	142.45	135.64	174.25	66.4	39.2
	<i>DMSO-d₆</i>	142.9	135.8	175.1	66.7	39.3
2	CHCl ₃	131.3	128.0	165.8	62.8	32.0
	<i>CHCl₃</i>	142.3	135.6	174.2	66.5	39.0
	<i>DMSO-d₆</i>	142.6	135.4	175.0	66.4	39.1
3	CHCl ₃	126.1	135.5	167.0	62.8	39.9
	<i>CHCl₃</i>	136.9	146.9	175.0	66.5	39.2
	<i>DMSO-d₆</i>	136.7	148.1	176.2	66.7	39.1
4	CHCl ₃	126.1	135.9	167.1	63.0	32.2
	<i>CHCl₃</i>	136.8	146.9	174.8	66.6	39.0
	<i>DMSO-d₆</i>	136.8	146.8	175.1	66.3	39.1

The carbonyl carbon atom C=O in the ^{13}C NMR spectra of the synthesized compounds resonates in the ranges of $\delta = 165.8\text{--}167.1$ ppm. This signal corresponds to the most downfield peak in the spectrum. The signals of the carbon atoms of the ethylene group ($\text{CH}=\text{CH}_2/\text{C}(\text{CH}_3)=\text{CH}_2$) of the compounds can be seen between $\delta = 126.1$ and 135.9 ppm. All the ^1H and ^{13}C NMR chemical shift values are within the range of the calculated values. Some deviations result from calculations in dimethyl sulfoxide instead of chloroform. It was a deliberate operation. The aim was to test whether a change in the solvent significantly affects the chemical shift values.

3.2. Vibrational Analysis

Infrared (IR) spectroscopy is a common and widely used spectroscopic technique employed due to its usefulness in determining structures of compounds and identifying them. Vibrational spectroscopy and quantum chemical calculations using the B3LYP functional and 6-311+G(d,p) basis set have been employed to study the structure of the title compounds. The most characteristic vibrational bands were collected in Table 3. The band characteristic of $\nu(\text{C}=\text{O})$ vibrations of ester fragments appeared in the range $1710\text{--}1721\text{ cm}^{-1}$. Moreover, the sharp bands of medium intensity at $1633\text{--}1635\text{ cm}^{-1}$ in the analyzed compounds were due to the stretching vibrations of the C=C group.

Table 3. Characteristic band strength values of the synthesized compounds.

Compounds	ν_s and ν_{as} (C–H)		ν_s and ν_{as} (C–H)	ν (C=O)	ν (C=C)
		or			
1	3032–3435		2889–2985	1720	1633
2	3035–3434		2880–2978	1721	1634
3	3060		2890–2953	1714	1635
4	3078–3408		2894–2976	1710	1635

The theoretical spectrograms for the IR spectra of the synthesized compounds were also constructed and compared with the experimental spectra. The computed vibrational frequencies of these molecules were found to be in good agreement with the experimental results (Figure 1).

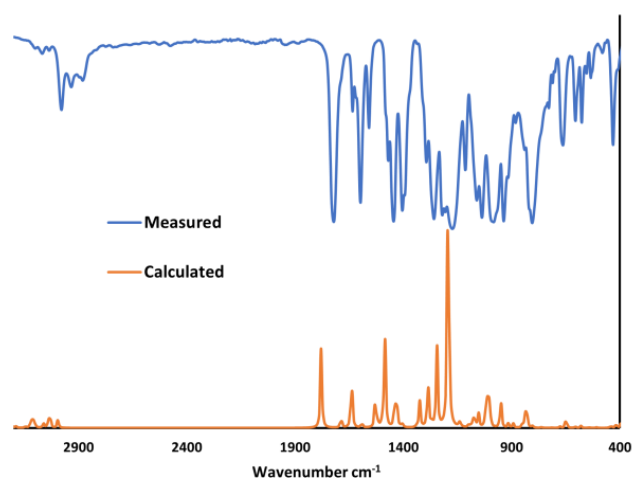


Figure 1. Comparison of the observed with simulated (scaled) IR spectra of 2-(2-(6-ethoxy benzothiazolyl)thio)ethyl acrylate (2).

3.3. Spectroscopic Studies

The data characterizing the spectroscopic properties of the synthesized compounds were presented in Table 4 and Figure 2.

Table 4. Measured and calculated spectroscopic data of 2-(2-benzothiazolythio)ethyl acrylate (1, 2) and methacrylate (3, 4) derivatives in selected solvents of different polarities.

Compound	Solvent	λ_{ab} (nm) (Measured)	λ_{ab} (nm) (Calculated)	ϵ ($\times 10^4, M^{-1} \cdot cm^{-1}$)	Direct Energy Band Gap (eV)
1	DCM	278	276	1.58	3.93
	MeOH	277	275	1.68	3.92
	DMSO	280	276	2.47	3.95
2	DCM	291	287	2.72	3.86
	MeOH	296	286	2.92	3.89
	DMSO	298	287	3.05	3.89
3	DCM	279	276	2.00	4.03
	MeOH	278	275	1.65	4.03
	DMSO	280	276	1.89	4.02
4	DCM	292	278	2.15	3.90
	MeOH	296	286	2.22	3.91
	DMSO	298	287	1.79	3.86

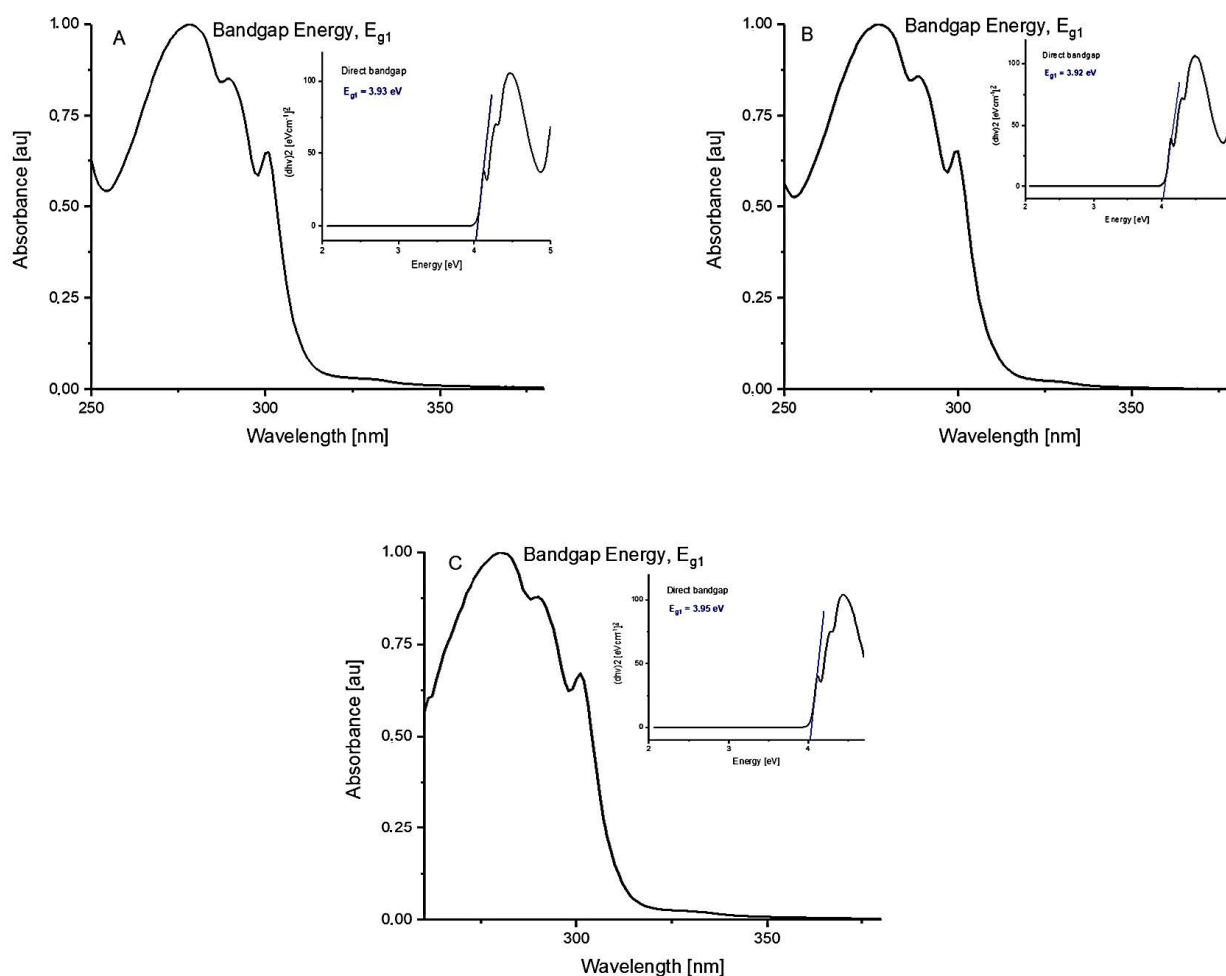


Figure 2. Tauc's plot of $(\alpha h\nu)^2$ as a function of photon energy ($h\nu$) for the 2-(benzothiazolythio)ethyl acrylate (1) in selected solvents of different polarities ((A) dichloromethane, (B) methanol, and (C) dimethyl sulfoxide).

As shown in Figure 3A, the compounds under study have a pronounced absorption band with the maximum (λ_{ab}) located in the range from 278 nm to 298 nm. The position of the absorption band depends on the polarity of the solvent. When the polarity increases, the absorption band slightly shifts toward a higher wavelength (bathochromic shift) from the non-polar dichloromethane (DCM) to the polar aprotic dimethyl sulfoxide (DMSO) (Figure 3B). The position of the absorption band depends not only on the solvent but also on the structure of the compound. The change from acrylic (compounds 1 and 2) to methacrylic (compounds 3 and 4) derivatives has no significant effect on the position of the absorption band. In this case, the location of the absorption band is the most affected by the presence of a substituent attached to the phenyl ring (Figure 3A). The introduction of the ethoxy substituent increases the electron density on the aromatic ring and results in the slight bathochromic shift (~19 nm) of the absorption spectra maxima. All the results were supported by calculations. The fluorescence properties (e.g., maximum of fluorescence, Stokes Shift, and fluorescence quantum yield) could not be determined because the tested compounds do not emit fluorescence under excitation at the absorption band maximum.

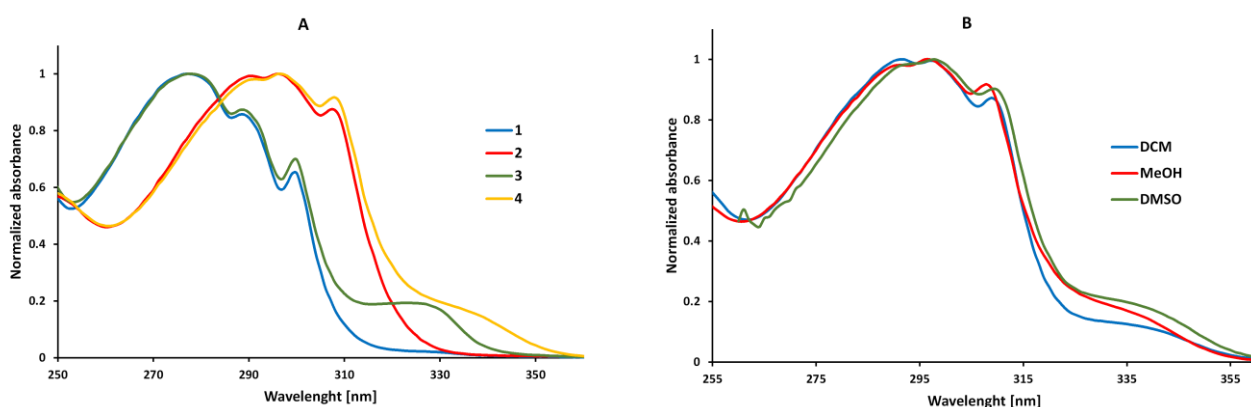


Figure 3. Normalized absorption spectra of 1–4 in methanol (A) and normalized absorption of 2-(2-(6-ethoxybenzothiazolyl)thio)ethyl methacrylate (4) in solvents of different polarities (B) (values were converted to have the maximum normalized at 1).

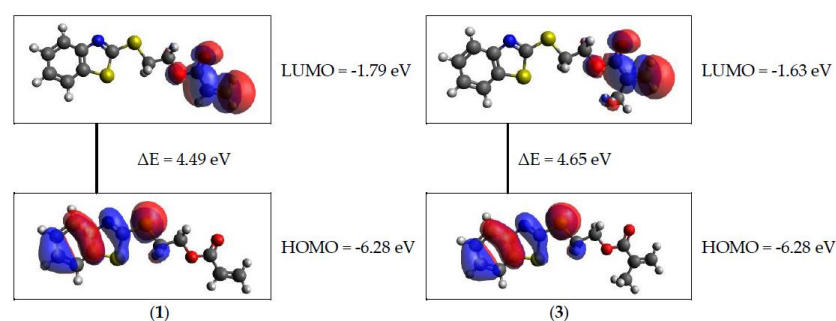
3.4. Computational Details

An important factor in assessing the practical use of the compounds under consideration is their reactivity. The most important orbital in molecules are the frontier molecular orbitals, called the Highest Occupied Molecular Orbital (HOMO) and Lowest Unoccupied Molecular Orbital (LUMO). The HOMO represents the ability to donate an electron, while LUMO, as an electron acceptor, represents the ability to accept an electron. The energy of the HOMO is directly related to the ionization potential, while the LUMO energy is directly related to the electron affinity [27]. The frontier molecular orbital energy gap helps to characterize the chemical reactivity and kinetic stability of the molecule. A molecule with a smaller energy gap between HOMO and LUMO is more polarizable and is generally associated with a high chemical reactivity, low kinetic stability, and is termed as a soft molecule [28–30]. In Table 5, there were presented values characterizing all the studied compounds, including energy values of HOMO and LUMO orbitals, energy gaps, and hardness (η).

Based on the obtained data, it can be concluded that among all the molecules under consideration, the derivatives containing the ethoxy substituent show the greatest reactivity. Such molecules were characterized by the lowest values of hardness and energy gap (Table 5). Moreover, the lower values of energy gap of 2-(2-benzothiazolylthio)ethyl acrylate derivatives (1, 2) may indicate that they are more reactive than 2-(2-benzothiazolylthio)ethyl methacrylate derivatives (3, 4) (Figure 4). No clear effect of the solvent polarity was observed on the calculated parameters.

Table 5. The values of hardness (η), energy gap, and energies of HOMO and LUMO orbitals estimated for all compounds.

Compound	Solvent	HOMO (eV)	LUMO (eV)	Energy Gap (eV)	η (eV)
1	DCM	-6.2811	-1.7943	4.4868	2.2434
	MeOH	-6.2882	-1.7878	4.5004	2.2502
	DMSO	-6.2893	-1.7872	4.5021	2.2510
2	DCM	-5.8727	-1.7894	4.0833	2.0416
	MeOH	-5.8871	-1.7845	4.1026	2.0513
	DMSO	-5.8890	-1.7839	4.1050	2.0525
3	DCM	-6.2806	-1.6335	4.6471	2.3235
	MeOH	-6.2871	-1.6332	4.6539	2.3269
	DMSO	-6.2879	-1.6327	4.6552	2.3276
4	DCM	-5.8713	-1.6250	4.2463	2.1231
	MeOH	-5.8868	-1.6278	4.2591	2.1295
	DMSO	-5.8885	-1.6294	4.2591	2.1295

**Figure 4.** Atomic orbital composition of the frontier molecular orbital for **1** (left) and **3** (right) in dichloromethane.

4. Conclusions

The selected 2-(2-benzothiazolylthio)ethyl acrylate (**1**, **2**) and methacrylate (**3**, **4**) derivatives were synthesized and their spectroscopic properties were characterized in three solvents of different polarities. The aim of the research was to check whether the modification of acrylate derivatives ($R^2 = H$ in Scheme 1) to methacrylate ($R^2 = CH_3$ in Scheme 1) would significantly affect the synthesis and spectroscopic properties of the new compounds. It has been shown that the performed modification had only a slight influence on the mentioned parameters. Only the modification of the structure of the molecule by the introduction of the ethoxy substituent results in the increase in the reactivity of the compound and in the slight bathochromic shift (~ 19 nm) of the absorption spectra maxima. The experimental data were supported by the quantum chemistry calculations, which not only reproduced the experimental trends but also contributed to the understanding of the electronic structure of the studied compounds.

Author Contributions: Conceptualization, J.K.-B. and A.S.; methodology, A.S.; software, A.S.; validation, J.K.-B. and A.S.; investigation, A.S.; ab initio calculations, A.S. and P.C.; resources, A.S.; data curation, A.S.; writing—original draft preparation, A.S.; writing—review, J.K.-B. and A.S.; funding acquisition, A.S. All authors have read and agreed to the published version of the manuscript.

Funding: This research was funded in part by National Science Centre, Poland, grant number 2022/06/X/ST4/00581. For the purpose of Open Access, the author has applied a CC-BY public copyright licence to any Author Accepted Manuscript version arising from this submission.

Institutional Review Board Statement: Not applicable.

Informed Consent Statement: Not applicable.

Data Availability Statement: Data is contained within the article.

Acknowledgments: This research was supported by PL-Grid Infrastructure (<http://www.plgrid.pl/en> (accessed on 27 January 2022)).

Conflicts of Interest: The authors declare no conflict of interest.

References

1. Tropp, J.; Mehta, A.S.; Ji, X.; Surendran, A.; Wu, R.; Schafer, E.A.; Reddy, M.M.; Patel, S.P.; Petty, A.J.; Rivnay, J. Versatile Poly(3,4-ethylenedioxythiophene) Polyelectrolytes for Bioelectronics by Incorporation of an Activated Ester. *Chem. Mater.* **2022**, *35*, 41–50. [[CrossRef](#)]
2. Jin, C.; Zeng, H.; Zhang, F.; Qiu, H.; Yang, Z.; Mutailipu, M.; Pan, S. Guanidinium Fluorooxoborates as Efficient Metal-free Short-Wavelength Nonlinear Optical Crystals. *Chem. Mater.* **2022**, *34*, 440–450. [[CrossRef](#)]
3. Asem, H.; Malmström, E. Polymeric Nanoparticles Explored for Drug-Delivery Applications. *ACS Symp. Ser.* **2018**, *1296*, 315–331.
4. Jiang, P.; He, Y.; Zhao, Y.; Chen, L. Hierarchical Surface Architecture of Hemodialysis Membranes for Eliminating Homocysteine Based on the Multifunctional Role of Pyridoxal 5'-phosphate. *ACS Appl. Mater. Interfaces* **2020**, *12*, 36837–36850. [[CrossRef](#)] [[PubMed](#)]
5. Zhang, Y.; Zhang, M.; Xu, X.; HH Chan, C.; Peng, H.; JT Hill, D.; Fu, C.; Fraser, J.; KWhittaker, A. Anti-Fouling Surfaces for Extracorporeal Membrane Oxygenation by Surface Grafting of Hydrophilic Sulfoxide Polymers. *Biomacromolecules* **2022**, *23*, 4318–4326. [[CrossRef](#)]
6. Keum, H.; Kim, J.Y.; Yu, B.; Yu, S.J.; Kim, J.; Jeon, H.; Lee, D.Y.; Im, S.G.; Jon, S. Prevention of bacterial colonization on catheters by a one-step coating process involving an antibiofouling polymer in water. *ACS Appl. Mater. Interfaces* **2017**, *9*, 19736–19745. [[CrossRef](#)]
7. Yeazel, T.R.; Becker, M.L. Advancing Toward 3D Printing of Bioresorbable Shape Memory Polymer Stents. *Biomacromolecules* **2020**, *21*, 3957–3965. [[CrossRef](#)]
8. Alizadehgiashi, M.; Nemr, C.R.; Chekini, M.; Pinto Ramos, D.; Mittal, N.; Ahmed, S.U.; Khuu, N.; Kelley, S.O.; Kumacheva, E. Multifunctional 3D-Printed Wound Dressings. *ACS Nano* **2021**, *15*, 12375–12387. [[CrossRef](#)]
9. Fan, S.; Chen, K.; Yuan, W.; Zhang, D.; Yang, S.; Lan, P.; Song, L.; Shao, H.; Zhang, Y. Biomaterial-Based Scaffolds as Antibacterial Suture Materials. *ACS Biomater. Sci. Eng.* **2020**, *6*, 3154–3161. [[CrossRef](#)]
10. Guan, X.; Wei, T.; Cai, J.; Sun, J.; Yu, S.; Guo, D. Poly(propylene fumarate)-Based Adhesives with a Transformable Adhesion Force for Suture-Free Fixation of Soft Tissue Wounds. *ACS Appl. Polym. Mater.* **2022**, *4*, 1855–1866. [[CrossRef](#)]
11. Klinge, U.; Klosterhalfen, B.; Öttinger, A.P.; Junge, K.; Schumpelick, V. PVDF as a new polymer for the construction of surgical meshes. *Biomaterials* **2002**, *23*, 3487–3493. [[CrossRef](#)] [[PubMed](#)]
12. Ratner, B.D. Polymeric Implants. *Polym. Sci. A Compr. Ref.* **2012**, *9*, 397–411. [[CrossRef](#)]
13. Bozukova, D.; Pagnouille, C.; Jérôme, R.; Jérôme, C. Polymers in modern ophthalmic implants—Historical background and recent advances. *Mater. Sci. Eng. R Rep.* **2010**, *69*, 63–83. [[CrossRef](#)]
14. Cramer, N.B.; Stansbury, J.W.; Bowman, C.N. Recent advances and developments in composite dental restorative materials. *J. Dent. Res.* **2011**, *90*, 402–416. [[CrossRef](#)]
15. Maitz, M.F. Applications of synthetic polymers in clinical medicine. *Biosurf. Biotribol.* **2015**, *1*, 161–176. [[CrossRef](#)]
16. Parra, F.; Vázquez, B.; Benito, L.; Barcenilla, J.; San Román, J. Foldable antibacterial acrylic intraocular lenses of high refractive index. *Biomacromolecules* **2009**, *10*, 3055–3061. [[CrossRef](#)]
17. Chisholm, B.J.; Pickett, J.E. Method of Making a High Refractive Index Optical Management Coating and the Coating. U.S. Patent 7,045,558 B2, 15 May 2006.
18. Cracium, L.; Polishchuk, O.; Schriver, G.W.; Hainz, R. High Refractive Index Monomers, Compositions and Uses Thereof. U.S. Patent 2008/0200582 A1, 21 August 2008.
19. Lee, C.; Yang, W.; Parr, R.G. Development of the Colle-Salvetti correlation-energy formula into a functional of the electron density. *Phys. Rev. B* **1988**, *37*, 785–789. [[CrossRef](#)] [[PubMed](#)]
20. Becke, A.D. Density-functional thermochemistry. III. The role of exact exchange. *J. Chem. Phys.* **1993**, *98*, 5648. [[CrossRef](#)]
21. Ong, B.K.; Woon, K.L.; Ariffin, A. Evaluation of various density functionals for predicting the electrophosphorescent host HOMO, LUMO and triplet energies. *Synth. Met.* **2014**, *195*, 54–60. [[CrossRef](#)]
22. Petersson, G.A.; Bennett, A.; Tensfeldt, T.G.; Al-Laham, M.A.; Shirley, W.A.; Mantzaris, J. A complete basis set model chemistry. I. The total energies of closed-shell atoms and hydrides of the first-row elements. *J. Chem. Phys.* **1988**, *89*, 2193–2218. [[CrossRef](#)]
23. Petersson, G.A.; Al-Laham, M.A. A complete basis set model chemistry. II. Open-shell systems and the total energies of the first-row atoms. *J. Chem. Phys.* **1991**, *94*, 6081–6090. [[CrossRef](#)]
24. Frisch, M.J.; Trucks, G.W.; Schlegel, H.B.; Scuseria, G.E.; Robb, M.A.; Cheeseman, J.R.; Scalmani, G.; Barone, V.; Petersson, G.A.; Nakatsuji, H.; et al. Gaussian 09, Revision A.02. Available online: <http://gaussian.com/g09citation/> (accessed on 7 December 2017).
25. Hanwell, M.D.; Curtis, D.E.; Lonie, D.C.; Vandermeersch, T.; Zurek, E.; Hutchison, G.R. Avogadro: An advanced semantic chemical editor, visualization, and analysis platform. *J. Cheminform.* **2012**, *4*, 17. [[CrossRef](#)] [[PubMed](#)]
26. Hioki, Y.; Shibata, M.; Otani, T.; Ichinosawa, A.; Uehara, H.; Sumiya, N.; Teruda, T. (Meth)acrylate Compound and Polymerizable Composition. Patent JP2017014213A, 19 January 2017.

27. Azhagiri, S.; Jayakumar, S.; Gunasekaran, S.; Srinivasan, S. Molecular structure, Mulliken charge, frontier molecular orbital and first hyperpolarizability analysis on 2-nitroaniline and 4-methoxy-2-nitroaniline using density functional theory. *Spectrochim. Acta Part A Mol. Biomol. Spectrosc.* **2014**, *124*, 199–202. [[CrossRef](#)]
28. Singh, P.; Reena; Kumar, A.; Gupta, A.; Patil, P.S. Spectroscopic investigation and density functional theory prediction of first and second order hyperpolarizabilities of 1-(4-bromophenyl)-3-(2,4-dichlorophenyl)-prop-2-en-1-one. *J. Mol. Struct.* **2022**, *1269*, 133807. [[CrossRef](#)]
29. Rauk, A. *Orbital Interaction Theory of Organic Chemistry*, 2nd ed.; Wiley-Interscience: New York, NY, USA, 2001.
30. Streitwieser, A.J. *Molecular Orbital Theory for Organic Chemists*; Wiley: New York, NY, USA, 1961.

Disclaimer/Publisher's Note: The statements, opinions and data contained in all publications are solely those of the individual author(s) and contributor(s) and not of MDPI and/or the editor(s). MDPI and/or the editor(s) disclaim responsibility for any injury to people or property resulting from any ideas, methods, instructions or products referred to in the content.